NUCLEON DECAY EXPERIMENTS: STATUS AND PROSPECTS

D. S. Ayres, Argonne National Laboratory
E. W. Beier, University of Pennsylvania
B. D'Ettorre Piazzoli, Universita di Torino
J. Ernwein, CEN - Saclay
T. K. Gaisser, Bartol Research Foundation
S. Seidel, University of Michigan
L. R. Sulak, Boston University

Summary

We survey the current status and future prospects of experiments to search for nucleon decay. Results from current experiments are summarized, and the background rejection capabilities of various techniques are described. We discuss the prospects for improved sensitivity in the new experiments that are now coming into operation, and the opportunities for the next generation of detectors.

Introduction

Our main goal in this paper is to survey the results from current experiments to search for nucleon decay, and to assess the prospects for future experimental progress in this field. The first generation experiments built specifically to search for nucleon decay have now evaluated the results of several kiloton-years of exposure. Figure 1 shows the increase of integrated exposure with time for the largest experiments. The lessons learned about the rejection of background from atmospheric neutrino interactions have led to new experiments (including upgrades of existing detectors) which are now coming into operation, and to proposals for larger and more powerful detectors which could be constructed in the future. Table 1 summarizes the several generations of experiments.

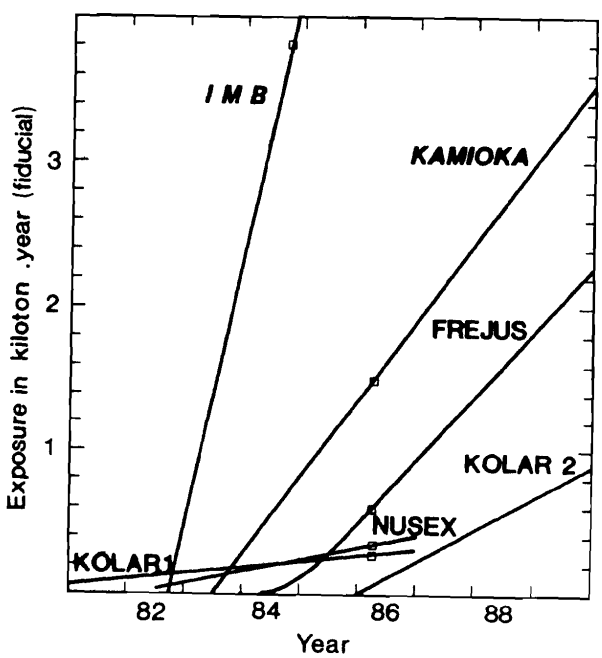

Fig. 1. Increase with time of the integrated exposure of the largest nucleon decay experiments.

Background Rejection

Sensitivity to nucleon decay requires not only a large mass and long exposure time, but also the ability to distinguish between background events and nucleon decay. In practice, the only important background is from the interactions of atmospheric neutrinos within a detector's active mass. The rate of these interactions is equivalent to a nucleon lifetime of about 1×10^{30} years in a detector with no background rejection capability. Background rejection is different for different detectors, and for a given detector also depends on the specific decay mode.

The typical experiment observes about 120 contained events in a kiloton-year of exposure, a rate which is consistent with expectations from neutrino interactions. The neutrino background is described in detail below. A subset of the contained events may satisfy cuts imposed to isolate nucleon decay. The number of these candidate events is typically a few percent of the number of contained events (for decay modes which do not involve neutrinos in the final state); individual candidate events often have a significant probability of having been due to a neutrino interaction, in addition to satisfying a nucleon decay hypothesis. As long as a given experiment can increase its exposure without observing candidate events in a given decay mode, its limit on the lifetime over branching ratio in that mode will increase proportional to the number of ton-years of exposure. As soon as an experiment reaches an exposure level where background events are observed (so that a background subtraction must be performed), the lifetime limit improves only as the square root of the exposure, and the experiment becomes background limited.

There are two types of detectors which have been used extensively to date: water Cerenkovs and tracking calorimeters. The water Cerenkovs were originally optimized to search for the decay mode $p \rightarrow e^+\pi^0$, which produces copious Cerenkov light and has a distinguishing back-to-back topology of electromagnetic showers. Monte Carlo simulations indicate that the background rejection for this and similar modes is excellent. Particle identification based upon ring images is fair, although not as good as in tracking calorimeters. Experimental results give no candidate events for this mode in the IMB and Kamiokande experiments at the current exposure level of 3×10^{32} nucleon years. The initial implementation of the water Cerenkov counters did not exploit the full sensitivity of the technique. The IMB detector had limited light collection and the Kamiokande detector was not instrumented to measure the time of the photomultiplier tube signals. Typically background events occurred at a few times 10^{31} years in most modes; this situation has motivated the recent upgrades of the IMB and Kamiokande experiments.

Tracking calorimeter detectors typically interleave accurate track detectors with finely segmented iron to obtain bubble-chamber-like reconstructions of events. They can in principle achieve better background rejection than the water Cerenkovs for decay modes with complex topologies and low-energy

particles. Particle identification is possible from dE/dx information, but track direction is more difficult to obtain than in the water Cerenkovs. The compact modular construction of most tracking calorimeters makes it relatively easy to measure their responses to charged particles and to neutrinos in accelerator test beams. Thus, efficiencies and background rejection can be determined more directly than for water Cerenkov detectors. Because tracking calorimeters are significantly more expensive per kiloton than the water Cerenkovs, there has been less experience with this technique to date in underground experiments. This situation is changing, however, with the commissioning of the 900 ton Frejus detector, which became fully operational in 1985.[8]

Table 1

Summary of experiments to search for nucleon decay. SC = scintillation counters, TC = tracking calorimeter, WC = water Cerenkov, LA = liquid argon TPC.

Experiment	Total Mass	Technique	Operation	Ref.
EARLY EXPERIMENTS:				
Homestake	300 tons	SC	1979 - 1981	1
KGF 1	140 tons	TC	1980 -	2
Soudan 1	30 tons	TC	1981 - 1983	3
FIRST GENERATION:				
NUSEX	150 tons	TC	1982 -	4
IMB 1	8000 tons	WC	1982 - 1984	5
HPW	700 tons	WC	1983 - 1985	6
Kamiokande 1	3000 tons	WC	1983 - 1985	7
SECOND GENERATION:				
Frejus	900 tons	TC	1984 -	8
IMB 2	8000 tons	WC	1984 -	9
KGF 2	260 tons	TC	1985 -	10
Kamiokande 2	3000 tons	WC	1986 -	11
Soudan 2	1100 tons	TC	construction	12
FUTURE:				
ICARUS 1	2000 tons	LA	R&D	13
ICARUS 2	20,000 tons	LA	proposal	13
Super-Kamiokande	46,000 tons	WC	proposal	14

Table 2

Summary of the parameters and the contained event rates of current nucleon decay experiments.

Group	KGF	NUSEX	Frejus	IMB	Kamiokande
First Operation	1980	1982	1984	1982	1983
Location	India	Alps (Italy)	Alps (France)	Ohio (USA)	Japan
Method	Iron + prop. counters	Iron + resist. streamer tubes	Iron + Geiger + flash cham.	Water Cerenkov	Water Cerenkov
Depth (hg/cm^2)	7600	5000[a]	4850[a]	1570	2700
Latitude (geogr.)	13°	46°	45°	42°	36°
Fiducial Mass (kton)	0.06	0.13	0.6	3.3	0.9
Exposure (kton-yr)	0.28	0.42	0.6	3.8	1.5
Contained Events	23	37	65	401	181
Rate (events/kton-yr)[b]	82	89	108	106	121
Expected Rate[c]	~ 60	88	100	106	113
Decay Candidates (non-ν modes)	3	3	1	21	5
Candid./Contained	13%	8%	1.5%	5%	3%

a. Average rock thickness traversed by muons which reach the detector.
b. Observed rate, not corrected for efficiencies and energy thresholds.
c. Taking into account efficiencies, energy thresholds, and latitude effects.

Proposals for future detectors have involved either exploitation of the well-understood water Cerenkov technique on a very large scale, as in Super-Kamiokande,[14] or the use of state-of-the-art time-projection techniques, as in ICARUS.[13] Neutrino backgrounds are more strongly rejected in these detectors than in the existing detectors, due to the finer granularity of the information. Super-Kamiokande has more than ten times as many photomultiplier tubes as the existing Kamiokande detector and the ICARUS detector resembles an electronic heavy liquid bubble chamber.

Summary of Experimental Results

Table 2 summarizes the important parameters of the most sensitive nucleon decay detectors, and compares the observed rates of candidate events and contained events. Table 3 gives the current lifetime-over-branching ratio limits for specific decay modes from these experiments. While the rate of contained events is consistent with the expected atmospheric neutrino background, the rate of candidate events limits the sensitivity in many modes. For these modes, it is clear that better background rejection, and better detectors, are needed.

Figure 2 compares the energy spectra observed for contained events with the expectations from interactions (in the detectors) of neutrinos produced by cosmic rays in the Earth's atmosphere. Table 4 gives the numerical fluxes expected for the sites of the current nucleon decay searches, taking into account geomagnetic effects on the primary spectrum characteristic of each site.[15] The curves in Fig. 2 have been calculated by each group taking into account the details of its detector efficiencies. Extended versions of Table 4 have been used as input for the curves in Fig. 2a, b, and c.

The effect of solar modulation on the primary spectrum is important only at low neutrino energies and so is not important for the nucleon decay background. The variation from solar minimum to solar maximum in the Northern U.S. is ± 12% from the average in the 0.2-0.4 GeV bin and is negligible above 0.8 GeV. The effect is smaller at the other sites because they are at lower geomagnetic latitude: ± 10%, 6%, and 5% in the 0.2-0.4 GeV energy bin respectively at NUSEX/Frejus, Kamiokande and KGF.

Uncertainties in the calculated fluxes arise from the uncertainty in the primary spectrum, uncertainty in the parametrization of particle production used in the Monte Carlo simulation to compute pion and kaon production and uncertainty in the geomagnetic cutoffs. The uncertainty in the primary spectrum has been investigated recently.[16] It leads to an overall uncertainty in the calculated fluxes of roughly ± 10%. Uncertainty arising from the parametrization of particle production is harder to estimate. Comparison of simultaneously calculated muon fluxes to measurements gives some constraint (but only limited because of the importance of muon energy loss in the atmosphere). This, together with comparisons with other calculations suggests an uncertainty of ± 10-15%. All calculations so far have used an offset dipole model of the geomagnetic field to calculate the cutoffs. According to Cooke[17] the true cutoffs can differ by as much as 40% in particular directions. Moreover there is a systematic underestimate of the cutoffs near the horizon for some azimuthal angles, which would lead to an overestimate of the calculated neutrino flux.

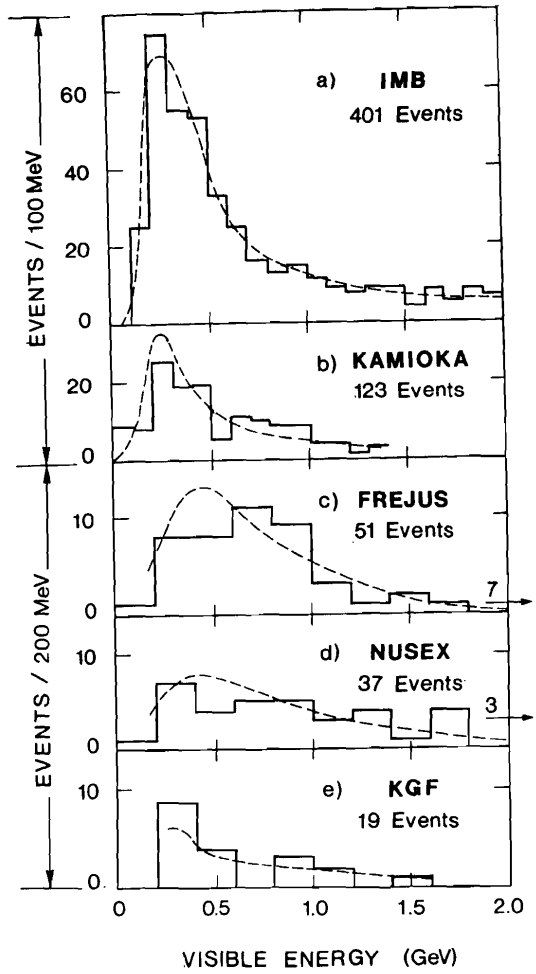

Fig. 2. Comparison of the energy spectra of contained events observed in nucleon decay experiments with the expectations from the interactions of atmospheric neutrinos in the detectors.

Overall uncertainty in the calculated neutrino fluxes is thus at least of order of ± 20%, and the best normalization of the calculations are the current measurements of neutrino interactions in the nucleon decay detectors as shown in Fig. 2. Calculated energy spectra and ratios of neutrino flavors are much less uncertain. With the possible exception of ν_e to ν_μ ratio, all aspects of contained event rates appear to be understood experimentally and in agreement with expectation, so that the calculated neutrino fluxes are not a source of uncertainty for the evaluation of the background for nucleon decay.

Status of Current Experiments

IMB

The IMB 1 detector[18] is a rectangular 8 kton water Cerenkov calorimeter located at a depth of 1580 mwe in Fairport Harbor, Ohio. The experiment is supported by a collaboration of groups from University of California - Irvine, University of Michigan, Brookhaven, Caltech, Cleveland State, Hawaii, University College London, and Warsaw University. Five inch photomultiplier tubes (PMT's) arranged on a 1 m wall grid record timing and pulse height information for triggers from cosmic rays and contained events, and delayed timing information for muon decay electron showers. The 2.8 Hz trigger rate is

Table 3

Partial lifetime limits from current nucleon decay experiments in units of 10^{31} yr (90% C.L.)

	IMB	Kamiokande	NUSEX	Frejus[a]
$p \to e^+\pi^0$	27.	11.3	0.8	6.
$e^+\eta^0$	20.	7.3	-	↑
$e^+\omega^0$	3.7	3.2	-	0.8 - 3.
$e^+\rho^0$	1.7	3.8	-	↓
e^+K^0	7.7	7.7	-	
$\mu^+\pi^0$	18.	8.6	0.9	6.
$\mu^+\eta^0$	4.9	2.8	-	↑
μ^+K^0	4.	2.9	0.9	0.8 - 3.
$\mu^+\rho^0$	1.6	2.3	-	↓
$\mu^+\omega^0$	2.3	2.1	-	
$n \to e^+\pi^-$	9.2	5.5	1.	6.
$e^+\rho^-$	3.2	1.7	-	
$\mu^+\pi^-$	3.2	4.2	0.9	6.
$\mu^+\rho^-$	0.7	0.8	-	-
$p \to \nu\pi^+$	-	0.6	0.2	-
$\nu\rho^+$	0.8	1.1	-	-
νK^+	1.	5.	1.1	-
$n \to \nu\pi^0$	0.6	5.9	1.4	-
$\nu\eta^0$	2.5	3.9	-	-
$\nu\omega^0$	1.2	2.7	-	-
$\nu\rho^0$	0.6	0.7	-	-
νK^0	1.5	4.3	1.2	-

a. Preliminary

dominated by through-going cosmic rays, which account for ~ 97% of all triggers. Contained events occur at a rate of about one per day and are consistent in absolute flux, spectrum, and directional distribution with models for atmospheric neutrino interactions. Data reduction techniques place upon contained events requirements in visible energy and unbalanced momentum determined from detailed signal and background simulations. In 417 live days of operation, twenty-one events were detected which satisfy criteria for nucleon decay modes with neutrinoless final states. These lead to 90% confidence level partial lifetime limits for 34 decay modes in the range 0.5-50 × 10^{31} years.[19]

In contrast to the thinking of a few years ago, recent theoretical interest in nucleon decay has often been focussed upon decay modes with isotropic final states such as those involving kaons and other heavy mesons.[20] The energy-momentum analysis retains a few candidates for most of these modes, for which it sets lifetime limits of a few × 10^{31} years. In order to better understand these many-prong modes, a new analysis technique has been implemented[21] which allows reconstruction of every track's visible energy and direction, with consequent reconstruction of the invariant mass and residual momentum of the nucleon and meson products. The technique is based upon automated recognition of local maxima in the energy deposition in the calorimeter. It achieves 15% resolution on the invariant masses and momentum resolution of the order of the Fermi smearing, and it allows reliable separation of overlapped tracks down to a 45° included angle. By using more of the available information, the method admits stricter topological cuts than were previously applied to events and leads to a consequent reduction in background. The number of candidates for accessible three-prong decay modes is cut from 17 to 3, and most three-prong lifetime limits are increased by factors of 2-4. Even on two-prong modes, the technique reduces the number of candidates by half. In an attempt to better distinguish signal from background, additional Q-pattern recognition studies are now underway to specify final state particle types.

The IMB detector recently underwent a series of upgrades in order to improve its event reconstruction capabilities. In the first phase, each 5 inch PMT was optically coupled to a 2-ft × 2-ft × 0.5-in acrylic plate which is doped with a waveshifting organic compound, bis-MSB, and mounted in the PMT plane. Light collection doubled as a fraction of the photons which would otherwise have missed a PMT were absorbed in a plate, trapped within it after reemission because of total internal reflection, and eventually propagated to the acrylic-PMT bulb (photocathode) interface. The detector was operated in Phase I upgrade mode for about 70 live days. Following this, a Phase II upgrade was initiated which involved replacement of all 5 inch PMT's by 8 inch ones and provided another factor of two increase in light collection. Data collection from Phase II began this summer, and preliminary results from both upgrades will be available shortly.

Kamiokande

The Kamiokande (Kamioka Nucleon Decay Experiment) detector is a water Cerenkov detector comprised of 3000 tons of water contained in a cylindrical steel tank and viewed by 1000 photomultiplier tubes of 20 inch diameter deployed on a 1 m grid on the inner surface of the cylinder. It is located in a mine 300 kilometers west of Tokyo at a depth of 2700 mwe. The University of Tokyo, University of Niigata, KEK collaboration began operating the detector in July, 1983. In 1985 the detector was upgraded by an expanded collaboration which includes the University of Pennsylvania and Caltech.[11] The upgrade consisted of surrounding the detector with a 4π hermetic, live anticounter and instrumenting the photomultipliers with multi-hit time and charge measuring electronics. The anticounter makes the selection of nucleon decay candidates quite simple, and the electronic upgrade improves the reconstruction resolution and therefore improves the rejection of background events induced by neutrinos. Specifically, for final states involving a charged lepton and a meson, Monte Carlo calculations indicate that the background rejection is improved by a factor of four. The upgraded detector has been operational since the start of 1986.

In 1.47 kiloton-years of operation the Kamioka detector has observed five candidates for nucleon decay.[22] Four of these events have a reasonable probability of being induced by neutrinos, but one of the events, a candidate for $p \to \mu^+\eta$, has an estimated background of 0.03 neutrino induced events at 90% confidence level. The upgraded Kamiokande II experiment is not yet background limited, and will continue to search for nucleon decay candidates. The detector also has contributed to the search for

magnetic monopoles, neutron-antineutron oscillation, astrophysical sources of underground muons, and has begun to search for neutrinos emitted by the sun.[23]

KGF

The Kolar Gold Field experiments are being performed by a collaboration of groups from the Tata Institute of Fundamental Research in Bombay, the Osaka City University in Osaka, and the Institute for Cosmic Ray Research at the University of Tokyo. The pioneering KGF 1 detector[2] has been operating since 1980, and has accumulated a total live time of 4.7 years to date. The KGF 2 experiment has been operating since December 1985. Both experiments make use of the same basic detector element, 10 cm by 10 cm steel-walled proportional tubes stacked in a crossed array to give two orthogonal views of each event. KGF 1 is 4 m by 6 m by 3.7 m high, with a total mass of 140 tons and a fiducial mass of 60 tons; KGF 2 is 6 m by 6 m by 6.5 m high, with a total mass of 260 tons and a fiducial mass of 150 tons. KGF 1 is located at a depth of 2300 m (7600 mwe), and KGF 2 is slightly shallower at 2000 m (6600 mwe). KGF 2 is surrounded on three sides by a 60-ton proportional tube veto shield and has a more sophisticated data acquisition system than KGF 1. The new cavity which was constructed for KGF 2 will also accommodate a future expansion to increase the size of the experiment by an additional factor of three.[10]

In its 4.7 years of live time, KGF 1 has observed four candidates for nucleon decay, three of which are for decay modes without neutrinos in the final state. The experiment has also observed two candidates for neutron-antineutron oscillations. The KGF group has operated a series of cosmic ray detectors at various depths prior to the construction of KGF 1, and has acquired data on a number of interesting cosmic ray topics. An important outstanding issue in cosmic ray physics is the nature of the so-called Kolar events, which are characterized by several charged particles originating from a vertex in the air surrounding a detector, perhaps due to the decay in flight of new, massive, long-lived particles. In addition to its increased sensitivity to nucleon decay, KGF 2 is expected to be particularly useful in studying Kolar events.

NUSEX

The Mont Blanc nucleon stability experiment (NUSEX) is a collaboration of groups from Frascati (INFN), Milan (INFN), Turin (CNR), and CERN. The detector is installed in the garage 17 in the road tunnel linking France and Italy at 45.8° N latitude. The rock thickness is known with high accuracy ($dh/h \sim 1\%$) at zenith angles $\theta < 75°$ and exceeds 4800 hg/cm^2 of standard rock in every direction. The detector is a digital tracking calorimeter consisting of 134 horizontal iron plates 3.5 × 3.5 m^2, 1 cm thick, interleaved with plastic streamer tubes 3.5 m long and 9 × 9 mm^2 in cross section. The gap between two iron plates is 1.7 cm so that the detector takes approximately the form of a cube with a total mass of 150 tons and average density of 3.5 g/cm^3. The tube walls are coated with graphite ($R \gtrsim 50$ kohm/square) to form a cathode which allows the signals produced to be picked up on external strips placed parallel and perpendicular to the wires. These strips provide the bidimensional readout with a single track point resolution of ~ 3 mm and ~ 4 mm respectively.

Table 4

Neutrino fluxes (ν's/(m^2 · sr · s · bin)) averaged over all directions and averaged over the solar cycle.

Site/Energy (GeV)	$\nu_e + \bar{\nu}_e$	$\nu_\mu + \bar{\nu}_\mu$
IMB (Northern U.S.)		
0.2-0.4	540.	1200.
0.4-0.6	180.	420.
0.6-0.8	83.	190.
0.8-1.0	44.	110.
1.0-1.2	27.	64.
1.2-1.4	17.	41.
1.4-1.6	11.	29.
1.6-1.8	7.9	20.
1.8-2.0	5.6	14.
2.0-3.0	13.	36.
> 3.0	9.7	30.
Kamiokande		
0.2-0.4	340.	750.
0.4-0.6	130.	300.
0.6-0.8	64.	150.
0.8-1.0	36.	87.
1.0-1.2	22.	54.
1.2-1.4	15.	36.
1.4-1.6	10.	26.
1.6-1.8	7.2	18.
1.8-2.0	5.2	14.
2.0-3.0	13.	35.
> 3.0	10.	30.
NUSEX/Frejus		
0.2-0.4	490.	1100.
0.4-0.6	170.	400.
0.6-0.8	80.	190.
0.8-1.0	43.	100.
1.0-1.2	26.	63.
1.2-1.4	17.	40.
1.4-1.6	11.	28.
1.6-1.8	7.8	20.
1.8-2.0	5.6	14.
2.0-3.0	13.	36.
> 3.0	9.6	30.
KGF (India)		
0.2-0.4	280.	630.
0.4-0.6	110.	250.
0.6-0.8	55.	130.
0.8-1.0	31.	76.
1.0-1.2	20.	48.
1.2-1.4	13.	32.
1.4-1.6	9.0	23.
1.6-1.8	6.4	17.
1.8-2.0	4.7	12.
2.0-3.0	12.	32.
> 3.0	9.2	29.

The pulses from the strips are discriminated and shaped to 7 μsec and are fed into a shift register chain. All signals from one plane are combined together to produce a fast OR signal used for trigger logic and timing information. The trigger logic requires at least two contiguous planes hit within 2 μsec, or three contiguous planes plus at least two contiguous planes, or at least three separated pairs of contiguous planes. This logic gives a trigger rate of ~ 170/day. About 26 triggers per day are due to cosmic ray muons, and the rest is due to rock and iron radioactivity. Atmospheric neutrinos produce about one trigger per month. The trigger efficiency for

nucleon decay is in the range 65-75% for decay channels with no energetic neutrino in the final state, and in the range 60-80% for neutrino interactions.

Each tube plane is equipped with a TDC with 100 nsec resolution: these are used to identify the delayed positron, emitted in the forward direction, from stopping μ^+ (35% efficiency). More details on the site and on the detector performance are given in Ref. 24. A test module, with the same structure as the detector, has been exposed to electron and pion beams for calibration, and to a neutrino beam in order to evaluate the neutrino background to nucleon decay.[25]

In 3.2 years live time, corresponding to an exposure of 416 ton-years in the fiducial volume (~ 130 tons, the outer layers of tubes being used to veto against incoming particles), 37 fully contained events have been observed. Considering all these events as due to neutrino interactions, 25 have been identified as ν_μ interactions, 11 as ν_e interactions, and 1 event as ambiguous. Correcting for overall detection efficiency a neutrino production rate of 133 ± 27 neutrino/kton-year is obtained, and a value 0.32 ± 0.14 for the ratio of ν_e to ν_μ interactions. The production rate is in good agreement with the expectation of ~ 143 events/kton-yr from atmospheric neutrino interactions.[15] The energy distribution for neutrino induced events is shown in Fig. 2d together with the expected rates. The visible energy has been corrected to account for unseen particles and pion absorption in flight.

This sample also contains possible nucleon decay events which can be searched for on the basis of their topology and kinematic reconstruction. A detailed list of these criteria and the resulting overall detection efficiency for different nucleon decay channels can be found in Ref. 26. Ten candidates were found in the $\nu\pi^+$ channel, consistent with the estimated background of 8.5 events from elastic ν_μ interactions; 1 candidate in the μ^+K^0 channel (neutrino background 0.15 ± 0.09), 1 in the $e^+\pi^0$ (neutrino background 0.25 ± 0.07), 1 in the $\mu^+\pi^-$ (neutrino background 0.36 ± 0.07). Limits on nucleon lifetime divided by branching ratio for different nucleon decay channels are summarized in Table 3.

Besides nucleon decay, the NUSEX apparatus is producing significant results in cosmic ray physics: possible detection of high energy muons from Cygnus X-3,[27] measurement of the muon intensity underground up to 10,000 hg/cm^2, and muon bundle rates to study the energy spectrum and nuclear composition of primary cosmic rays,[28] determination of the prompt muon contribution to the atmospheric intensity to set a limit on the open charm hadroproduction cross section in the 50-100 TeV region.[29] The NUSEX experiment is planned to run at least until the end of 1987.

Frejus

The Frejus experiment is a collaboration of groups from Aachen, Orsay, Ecole Polytechnique, Saclay and Wuppertal. The detector is installed in an underground laboratory near Modane, France, at a depth of 4850 mwe. It is the first large underground "second generation" detector of the tracking calorimeter type. Its mass is 900 tons, its average density 2 g/cm^3, and it is made of a 912-layer sandwich of 3 mm thick iron plates and (5 × 5) mm^2 plastic flash tubes. The trigger for these flash chambers is provided by planes of Geiger tubes (15 × 15) mm^2 in cross section, encountered every 8 flash chamber planes. The vertical iron and detector planes (6 × 6 m^2) are hanging from a steel structure, and the tubes, which are alternately vertical and horizontal, provide two orthogonal views.

The trigger logic requires grouped hits in a small volume typical of nucleon decay events. The trigger rate is ≈ 50/hour and is mainly due to atmospheric muons (≈ 20/hour) and local radioactivity. The trigger efficiency for quasi-elastic neutrino interactions above 250 MeV/c is 75% and the efficiency to trigger on nucleon decays with a charged lepton is 85%. This efficiency drops to 30-60% for decay modes with a neutrino. The spatial resolution is 5 mm, and the momentum resolution is $\sigma(p)/p = 0.15/\sqrt{p}$ for electrons, 3% and 25% for 300 MeV/c muons and pions respectively. The fine sampling gives further information on $e/\mu/\pi$ separation and track direction.

The present exposure is 607 ton-year in the fiducial volume which is defined, in this preliminary analysis, by excluding a 50 cm wide peripheral region from each of the six detector faces. From 65 neutrino events produced in the fiducial volume and the 75% detection efficiency, a neutrino production rate of 143 ± 25 is obtained for $E_\nu > 250$ MeV. The ratio ν_e/ν_μ for charged current events is 0.52 ± 0.14 ± 0.10. The energy distribution of the 51 fully contained events is shown in Fig. 2c.

The search for nucleon decays with a charged lepton has been done by requiring the contained events to have their total energy around the nucleon mass and the momentum balance to be satisfied within limits defined by Fermi motion, nuclear interactions of final states hadrons, and measurement errors. Among 2-prong events, none can be considered as a nucleon decay candidate whereas one 3-prong event is kinematically compatible with a nucleon decay. This event also has several background interpretations (neutrino interaction). Only after detailed background studies will it be possible to make an accurate statement on how likely it is for this event to be nucleon decay and whether or not the experiment begins to be background limited for 3-prong events. This background study is in progress and uses data of low energy neutrino interactions of the Aachen-Padova experiment at CERN[30] as well as a detailed Monte Carlo simulation of neutrino interactions in the detector. These background studies also need to be completed before results on decay modes with a neutrino can be obtained. The partial lifetime limits which are given in Table 3 (Frejus) take into account the exposure, the average trigger efficiencies, and a very preliminary overall identification probability (including nuclear reinteraction). These limits are 6×10^{31} yr for decays with a charged lepton and one pion, and (0.8 to 3) × 10^{31} yr for decays with a charged lepton and ≥ 2 pions.

The full capabilities of the Frejus experiment will be exploited within two years when the exposure will be at least three times the present value (Fig. 1) and when the detailed background studies are completed. Besides nucleon decay, other physics topics are being investigated with the Frejus detector: underground muons from celestial point sources,[31] and muon bundles to study the chemical composition of primary cosmic rays.[32]

Future Prospects

In the immediate future we can expect a steady improvement of the lifetime limits from IMB and Kamiokande for those modes which are not background limited. The recent upgrades of these two experiments

will undoubtedly allow the background-limited lifetime levels to be pushed higher than would have been possible with the original detectors. Progress can also be expected from the improvement of analysis techniques, as illustrated by the recent results from IMB. In addition, the lifetime limits from the water Cerenkovs will soon be checked by completely independent results from the new calorimetric detectors (Frejus and Soudan 2) using a very different complementary technique.

The experience with the first generation of water Cerenkov detectors is probably a reasonable model for what can be expected from the large tracking calorimeters: despite careful Monte Carlo simulations at the design stage, the background rejection finally achieved will depend upon analysis techniques developed for the events which are actually observed. As with the water Cerenkovs, hardware upgrades may further improve the performance of the tracking calorimeters after some years of experience. The exploitation of the existing detectors will be a slow process, and it is difficult to predict at what lifetime level background processes will ultimately limit sensitivity for most decay modes, even for the relatively well understood water Cerenkovs.

Recent proposals to construct new large underground experiments for the real-time detection of solar neutrino interactions may have an important effect on the search for nucleon decay. The feasibility of water Cerenkov solar neutrino experiments is being tested in the Kamiokande detector, which was originally designed for nucleon decay. The instrumentation of a very large scale water Cerenkov detector[33] for solar neutrino detection may be more powerful than is required to search for nucleon decay. If such experiments are built, their large masses and excellent event-reconstruction capabilities will thus make possible searches for nucleon decay at the fundamental limits allowed by this technique.

Similarly, the ICARUS program involves the development of an important new technique for the detection of nucleon decay, and its eventual implementation in an extremely large detector. The very substantial investment required to carry out this program is primarily justified by the search for nucleon decay, but important additional motivation is being provided by low energy neutrino physics.

It is tempting to speculate that this cycle will continue: techniques developed for one type of underground physics will open up capabilities in related fields and lead to further improvements in detector capabilities. Until recently the justification for the investment required has been provided by the search for nucleon decay; the motivation for future progress may also include the study of solar neutrinos, cosmic ray phenomena, neutrino astronomy, or magnetic monopoles. If this process continues, the search for nucleon decay may well be pushed to the limits of sensitivity which are imposed by the constraints of the neutrino background, and our opportunity to study this fundamental process will be extended to even longer lifetimes than seemed possible a few years ago.

References

1. M. L. Cherry et al., Phys. Rev. Lett. 47, 1507 (1981).
2. M. R. Krishnaswamy et al., Phys. Lett. 106B, 339 (1981), and Phys. Lett. 115B, 349 (1982); M. R. Krishnaswamy et al., Proc. 6th Workshop on Grand Unif. (World Scientific, 1986), ed. by S. Rudaz and T. Walsh, p. 97.
3. J. Bartelt et al., Phys. Rev. Lett. 50, 651 (1983), and Phys. Rev. D (to be published).
4. G. Battistoni et al., Phys. Lett. 118B, 461 (1982).
5. R. M. Bionta, Phys. Rev. Lett. 51, 27 (1983); B. G. Cortez, Phys. Rev. Lett. 52, 1092 (1984); H. S. Park, Phys. Rev. Lett. 54, 22 (1985).
6. T. J. Phillips, "A Search for Nucleon Decay with Multiple Muon Decays," Harvard University Ph. D. Thesis, March 1986 (unpublished).
7. K. Arisaka et al., Journal of the Physical Society of Japan, 54, 3213 (1985).
8. J. Ernwein, Proc. 6th Workshop on Grand Unif. (World Scientific, 1986) ed. by S. Rudaz and T. Walsh, p. 25; R. Barloutaud, to appear in Proc. 7th Workshop on Grand Unif., Toyama, Japan (World Scientific Pub.), ed. by J. Arafune and K. Takahashi.
9. M. Goldhaber, rapporteur's talk at the XXIII Int. Conf. on High Energy Physics, Berkeley, CA, July 1986.
10. V. S. Narasimham, paper presented at the XXIII Int. Conf. on High Energy Physics, Berkeley, CA, July 1986.
11. E.W. Beier, to appear in Proc. 7th Workshop on Grand Unif., Toyama, Japan (World Scientific Pub.) ed. by J. Arafune and K. Takahashi.
12. J. L. Thron, ibid.
13. D. B. Cline, these proceedings.
14. Y. Totsuka, to appear in Proc. of the 7th Workshop on Grand Unif., Toyama, Japan (World Scientific Pub.), ed. by J. Arafune and K. Takahashi.
15. T.K. Gaisser, T. Stanev, S.A. Bludman and H. Lee, Phys. Rev. Lett. 51, 223 (1983); T.K. Gaisser and T. Stanev, Proc. 6th Workshop on Grand Unif. (World Scientific, 1986) ed. by S. Rudaz and T. Walsh, p. 236; and T.K. Gaisser, T. Stanev and G.D. Barr, in preparation.
16. G. Barr and T.K. Gaisser, Soudan 2 internal note PDK-281, Oxford, May 1986.
17. D.J. Cooke, Phys. Rev. Lett. 51, 320 (1983).
18. R. M. Bionta et al., Proc. Fermilab Workshop on Calorimeter Calibration (1983).
19. H. S. Park et al., Phys. Rev. Lett. 54, 853 (1985).
20. For an overview, see W. Marciano, these proceedings.
21. S. Seidel, Ph.D. thesis, Univ. of Michigan.
22. T. Suda, to appear in Proc. 7th Workshop on Grand Unif., Toyama, Japan (World Scientific Pub.), ed. by J. Arafune and K. Takahashi.
23. E. W. Beier, these proceedings.
24. G. Battistoni et al., Nucl. Instr. Meth. A245, 277 (1986).
25. G. Battistoni et al., Nucl. Instr. Meth. 219, 300 (1984).
26. G. Battistoni et al., Proc. 6th Workshop on Grand Unif. (World Scientific, 1986), ed. by S. Rudaz and T. Walsh, p. 11.
27. B. D'Ettorre Piazzoli, Proc. 19th ICRC, La Jolla, 9, 455 (1985).
28. G. Bologna et al., Nuovo Cimento C8, 76 (1985).
29. G. Battistoni et al., Nuovo Cimento C9, 196 (1986).
30. H. Faissner et al., Phys. Rev. D21, 555 (1980).
31. Ch. Berger et al., Phys. Lett. B174, 118 (1986); L. Moscoso, paper presented at the XXIII Int. Conf. on High Energy Physics, Berkeley, CA, July 1986; G. Chardin, to appear in Proc. of the NARW on High Energy Gamma Astronomy, Durham, England, August 1986.
32. S. Tisserant, paper presented at the XXIII Int. Conf. on High Energy Physics, Berkeley, CA, July 1986.
33. S. Seidel and L. Sulak, these proceedings.